

Selective destabilization of polypeptides synthesized from NMD-targeted transcripts

Vincent Chu^{a,b}, Qing Feng^{a,†}, Yang Lim^c, and Sichen Shao^{a,*}

^aDepartment of Cell Biology, Harvard Medical School, Blavatnik Institute, Boston, MA 02115; ^bDepartment of Chemistry and Chemical Biology, Harvard University, Cambridge, MA 02138; ^cDepartment of Biological Chemistry and Molecular Pharmacology, Harvard Medical School, Blavatnik Institute, Boston, MA 02115

ABSTRACT The translation of mRNAs that contain a premature termination codon (PTC) generates truncated proteins that may have toxic dominant negative effects. Nonsense-mediated decay (NMD) is an mRNA surveillance pathway that degrades PTC-containing mRNAs to limit the production of truncated proteins. NMD activation requires a ribosome terminating translation at a PTC, but what happens to the polypeptides synthesized during the translation cycle needed to activate NMD is incompletely understood. Here, by establishing reporter systems that encode the same polypeptide sequence before a normal termination codon or PTC, we show that termination of protein synthesis at a PTC is sufficient to selectively destabilize polypeptides in mammalian cells. Proteasome inhibition specifically rescues the levels of nascent polypeptides produced from PTC-containing mRNAs within an hour, but also disrupts mRNA homeostasis within a few hours. PTC-terminated polypeptide destabilization is also alleviated by depleting the central NMD factor UPF1 or SMG1, the kinase that phosphorylates UPF1 to activate NMD, but not by inhibiting SMG1 kinase activity. Our results suggest that polypeptide degradation is linked to PTC recognition in mammalian cells and clarify a framework to investigate these mechanisms.

Monitoring Editor

Karsten Weis
ETH Zurich

Received: Aug 6, 2021

Revised: Sep 13, 2021

Accepted: Sep 24, 2021

INTRODUCTION

Mutations or mRNA processing events that introduce a premature termination codon (PTC) in an mRNA can result in the production of truncated proteins that perturb protein homeostasis by aggregating or performing dominant negative functions. To limit production of deleterious truncated proteins, eukaryotic cells employ the nonsense-mediated mRNA decay (NMD) pathway to degrade PTC-containing mRNAs (Chang and Kan, 1979; Losson and Lacroute, 1979;

Maquat *et al.*, 1981; Kurosaki *et al.*, 2019; Yi *et al.*, 2021). NMD also regulates the expression of many normal genes, for example by degrading splice isoforms that contain an in-frame PTC or transcripts with upstream open reading frames (Mendell *et al.*, 2004; Saltzman *et al.*, 2008; Weischenfeldt *et al.*, 2012; Nasif *et al.*, 2018; García-Moreno and Romão, 2020).

Activating NMD requires translation, specifically a ribosome terminating protein synthesis at a PTC, which is distinguished from normal termination events by context (Belgrader *et al.*, 1993; Carter *et al.*, 1995; Lykke-Andersen *et al.*, 2000). The best predictor of an NMD target transcript is a splice site that leads to the deposition of an exon junction complex (EJC) ~50–55 nucleotides downstream of a termination codon (Nagy and Maquat, 1998; Singh *et al.*, 2008; Lindeboom *et al.*, 2019). Because EJCs are usually located within open reading frames and removed by translating ribosomes (Dostie and Dreyfuss, 2002; Gehring *et al.*, 2009; Saulière *et al.*, 2012; Hauer *et al.*, 2016), the presence of an EJC after a termination codon is a clear signal that the mRNA is aberrant. Another feature that can trigger NMD is a long 3' untranslated region (UTR) between the termination codon and poly(A) tail, although the length required is unclear and some long 3' UTRs contain sequences that evade NMD (Bühler *et al.*, 2006; Eberle *et al.*, 2008; Singh *et al.*, 2008; Toma *et al.*, 2015).

This article was published online ahead of print in MBoC in Press (<http://www.molbiolcell.org/cgi/doi/10.1091/mbc.E21-08-0382>).

[†]Current address: Department of Biology, Massachusetts Institute of Technology, 31 Ames St., Cambridge, MA 02139.

*Address correspondence to: Sichen Shao (sichen_shao@hms.harvard.edu).

Abbreviations used: dFP, dual fluorescent protein; DTT, dithiothreitol; EJC, exon junction complex; FBS, fetal bovine serum; FVβ, a model protein consisting of a 3xFLAG tag, the villin headpiece (VHP) domain, and the unstructured cytosolic region of Sec61β; IT, immunoprecipitation; NMD, nonsense-mediated decay; PBS, phosphate-buffered saline; PTC, premature termination codon; RQC, ribosome-associated quality control; TPI, triosephosphate isomerase; UTR, untranslated region.

© 2021 Chu *et al.* This article is distributed by The American Society for Cell Biology under license from the author(s). Two months after publication it is available to the public under an Attribution–Noncommercial–Share Alike 4.0 International Creative Commons License (<https://creativecommons.org/licenses/by-nc-sa/4.0>).

“ASCB®,” “The American Society for Cell Biology®,” and “Molecular Biology of the Cell®” are registered trademarks of The American Society for Cell Biology.

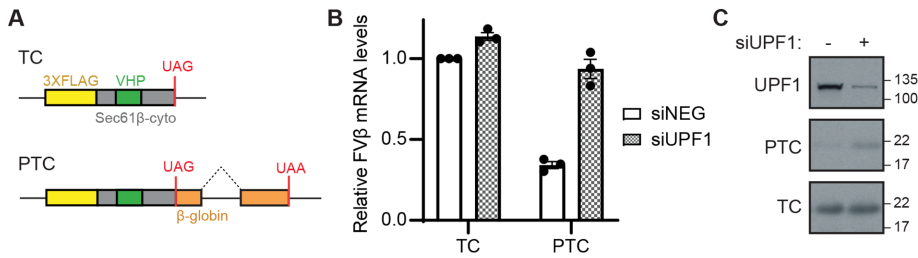


FIGURE 1: Matched reporters to study normal and premature translation termination. (A) FV β reporter design scheme. Identical protein sequences (FV β) comprising a 3xFLAG tag (yellow) and the autonomously folding VHP (green) domain embedded in the cytosolic portion of Sec61 β (up to valine 68; gray) are placed before a termination codon (UAG) that either is (PTC) or is not (TC) upstream of the β -globin gene sequence following amino acid 39 (orange). Dashed line, constitutive splice site. (B) Flp-In T-REx HEK293 cells stably expressing either the FV β -TC or FV β -PTC reporter were treated with a negative control siRNA (siNEG) or siRNA against UPF1 (siUPF1) for 72 h, and reporter expression was induced with 10 ng/ml doxycycline for 24 h. FV β reporter mRNA levels were measured by RT-qPCR and normalized to siNEG FV β -TC. Shown are mean \pm SEM for three replicates. (C) Reporter cells as in B were lysed and analyzed by SDS-PAGE and immunoblotting for UPF1 or the indicated Flag-tagged reporter protein. A representative blot of UPF1 knockdown efficiency is shown from FV β -TC reporter cell lysates.

Regardless of the feature(s) that distinguish a PTC, NMD activation converges on the phosphorylation of UPF1, an RNA helicase considered to be the central effector of NMD, by the protein kinase SMG1 (Ohnishi *et al.*, 2003; Kashima *et al.*, 2006; Okada-Katsuhata *et al.*, 2012). UPF1 and SMG1 are recruited directly or indirectly to PTC-containing mRNAs by factors associated with terminating ribosomes, EJCs, nascent mRNAs, and/or 3' UTRs (Le Hir *et al.*, 2001; Kashima *et al.*, 2006; Hogg and Goff, 2010; Hwang *et al.*, 2010). UPF1 phosphorylation leads to the recruitment of SMG6, an endonuclease that cleaves the mRNA near the PTC and the SMG5/SMG7 complex, which recruits the 5' decapping complex and the CCR4/NOT deadenylation complex (Ohnishi *et al.*, 2003; Okada-Katsuhata *et al.*, 2012; Cho *et al.*, 2013; Jonas *et al.*, 2013; Loh *et al.*, 2013; Boehm *et al.*, 2014; Chakrabarti *et al.*, 2014; Schmidt *et al.*, 2015; Ottens *et al.*, 2017). Together, these activities enable 3' to 5' mRNA degradation by the exosome and 5' to 3' mRNA degradation by the exonuclease XRN1 (Huntzinger *et al.*, 2008; Eberle *et al.*, 2009; Lykke-Andersen *et al.*, 2014; Schmidt *et al.*, 2015).

Although the degradation of PTC-containing mRNAs is well studied, less is known about what happens to the polypeptides synthesized during the translation cycle required to activate NMD. Several studies in yeast and mammalian cells suggest that the protein products of an mRNA with a PTC are less stable than proteins synthesized from an mRNA with a termination codon in a normal context (Kuroha *et al.*, 2009, 2013; Pradhan *et al.*, 2021; Udy and Bradley, 2021). In addition, when proteasomes are inhibited in mammalian cells, UPF1 may facilitate the targeting of truncated proteins produced by a PTC-containing mRNA to aggresomes that are eventually degraded by autophagy (Park *et al.*, 2020). Currently, the strongest links between NMD and post-translational protein destabilization are based on comparisons of truncated protein sequences with longer full-length protein sequences that may have different intrinsic stabilities. Thus, a key question that remains incompletely answered is whether the context of a PTC is sufficient to target protein products of defined sequences for degradation in mammalian cells.

In this study, we establish mammalian cellular reporters that encode the same protein sequence before normal termination codons or PTCs for quantitative comparisons of protein stability. Using independent biochemical and fluorescence-based assays, we present evidence that proteins synthesized from PTC-containing mRNAs are

selectively destabilized during or after translation. The destabilization of proteins produced from PTC-containing mRNAs is specifically rescued by proteasome inhibition or by depleting UPF1 or SMG1, but not by inhibiting SMG1 kinase activity. Our results support a functional connection between PTC recognition and protein degradation and highlight experimental parameters that should be considered when analyzing these mechanisms.

RESULTS

Matched reporters that terminate translation in different contexts

To evaluate how PTC recognition affects protein fate, we designed pairs of reporter constructs that encode the same protein sequence, but only one in each pair contains an intron after the termination codon to trigger EJC-dependent NMD (Figure 1A). Throughout this study, we refer to the reporter whose mRNA undergoes NMD as PTC and the matched reporter whose mRNA is not degraded by NMD as TC. The first protein sequence we analyzed is a biochemically characterized model protein (referred to as FV β) consisting of a 3xFLAG tag, the rapidly folding villin headpiece (VHP) domain, and the unstructured cytosolic region of Sec61 β (Shao *et al.*, 2013, 2015, 2016). We appended the genomic sequence of β -globin following codon 39, which contains an intron, after the termination codon of the FV β -PTC reporter construct. A nonsense mutation at codon 39 of the β -globin gene is linked to β -thalassemia, and the resulting transcript is well-established to be degraded by NMD (Lim *et al.*, 1989; Carter *et al.*, 1995; Ishigaki *et al.*, 2001; Trcek *et al.*, 2013).

We generated Flp-In T-REx 293 cell lines stably expressing either FV β -TC or FV β -PTC under an inducible promoter and validated that FV β -PTC mRNA undergoes NMD by assaying reporter protein and mRNA levels without and with siRNA-mediated knockdown of UPF1. Consistent with an NMD substrate, FV β -PTC mRNA and protein levels were lower than those of FV β -TC, as measured by RT-qPCR and immunoblotting, respectively (Figure 1, B and C). UPF1 knockdown selectively increased the protein and mRNA levels of FV β -PTC but not FV β -TC. Thus, FV β -PTC and FV β -TC are matched reporters to specifically analyze how premature termination affects protein fate.

UPF1 phosphorylation leads to the recruitment of SMG6, an endonuclease that cleaves the mRNA near the PTC and the SMG5/SMG7 complex, which recruits the 5' decapping complex and the CCR4/NOT deadenylation complex (Ohnishi *et al.*, 2003; Okada-Katsuhata *et al.*, 2012; Cho *et al.*, 2013; Jonas *et al.*, 2013; Loh *et al.*, 2013; Boehm *et al.*, 2014; Chakrabarti *et al.*, 2014; Schmidt *et al.*, 2015; Ottens *et al.*, 2017). Together, these activities enable 3' to 5' mRNA degradation by the exosome and 5' to 3' mRNA degradation by the exonuclease XRN1 (Huntzinger *et al.*, 2008; Eberle *et al.*, 2009; Lykke-Andersen *et al.*, 2014; Schmidt *et al.*, 2015).

Proteasome inhibition selectively stabilizes prematurely terminated proteins

To assay how translation termination at a PTC affects protein stability, we first investigated if proteasome inhibition affected the matched FV β -PTC and FV β -TC reporters. We treated the reporter cell lines with a mixture of 0.5 μ M bortezomib and 0.5 μ M epoxomicin to specifically target multiple proteolytic activities of the proteasome (Kisselev and Goldberg, 2001; Nguyen *et al.*, 2017). After 4 h of treatment with bortezomib/epoxomicin, FV β -TC protein levels were unchanged while FV β -PTC protein levels increased by \sim 1.8-fold (Figure 2A). Consistent with successful proteasome inhibition, polyubiquitinated protein levels also increased in the bortezomib/epoxomicin-treated cells (Figure 2A). However, the observation that FV β -PTC mRNA levels nearly doubled and FV β -TC mRNA levels decreased by \sim 30% over the course of the treatment precluded interpretations attributing the differences in protein levels specifically to proteasomal degradation (Figure 2B).

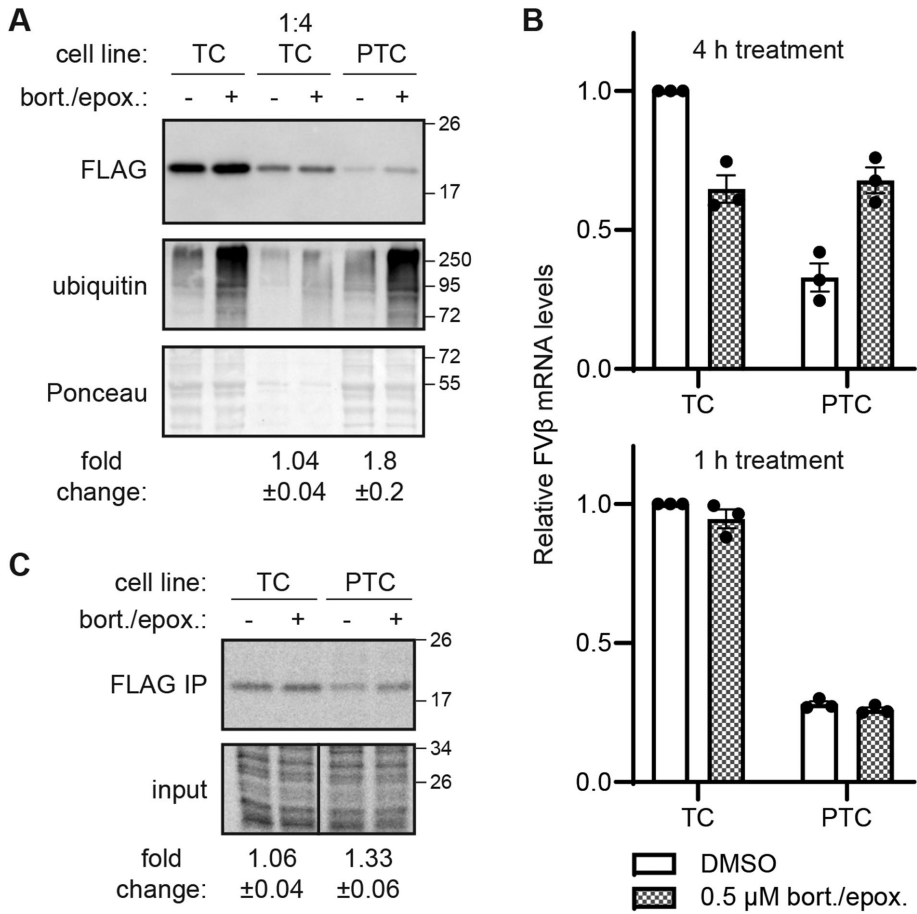


FIGURE 2: Effects of proteasome inhibition on reporter protein and mRNA levels. (A) FVβ-TC or FVβ-PTC expression was induced in Flp-In T-REx HEK293 cells with 10 ng/ml doxycycline for 24 h without or with 0.5 μM bortezomib and 0.5 μM epoxomicin (bort./epox.) for 4 h. Cell lysates normalized for total protein content were analyzed by SDS-PAGE and immunoblotting for the indicated factors. To facilitate comparison of reporter levels at similar ranges of chemiluminescence, FVβ-TC reporter cell lysates also were diluted fourfold (1:4). The mean fold change ± SEM in the FLAG signal for each reporter with proteasome inhibition is listed below for three replicates. (B) FVβ-TC or FVβ-PTC reporter cells were treated without or with bort./epox. for 4 (top) or 1 (bottom) h. FVβ reporter mRNA levels were measured by RT-qPCR and normalized to untreated FVβ-TC values. Shown are mean ± SEM for three replicates. (C) FVβ-TC or FVβ-PTC reporter cells were labeled with ~20.5 μCi [³⁵S]-methionine without or with bort./epox. for 1 h. Cell lysates were subjected to denaturing IPs for the FLAG-tagged reporter proteins (FLAG IP). FVβ-TC reporter cell lysates were diluted fourfold before IPs. Lysates (input) and IPs were analyzed by SDS-PAGE and autoradiography, and quantified by phosphorimaging. The mean fold change ± SEM of FVβ reporter levels with proteasome inhibition is listed below for three replicates.

The effects of proteasome inhibition on PTC mRNA levels were not isolated to the bortezomib/epoxomicin mixture or to reporters incorporated into the Flp-In locus. We observed similar changes in PTC reporter mRNA levels with transient transfections in HEK293 cells, and with 4 h of treatment with less specific proteasome inhibitors such as 10 μM MG132 or 10 μM lactacystin (Supplemental Figure S1, A and B), experimental conditions that are commonly used. These effects do not depend on the FVβ coding sequence, as replacing the FVβ open reading frame with that of superfolder GFP (sfGFP) resulted in the same trends in PTC mRNA levels after inhibitor treatment (Supplemental Figure S1C). In comparison, the decrease in FVβ-TC mRNA levels was not consistently observed with different proteasome inhibitors and reporter sequences. In addition, while proteasome inhibition preferentially increased PTC reporter mRNA

levels, the E1 inhibitor MLN7243 increased both FVβ-TC and FVβ-PTC mRNA levels. Prolonged proteasome inhibition has been reported to deplete cellular free ubiquitin levels, inhibit translation, and alter cellular signaling pathways (Mimnaugh *et al.*, 1997; Cowan and Morley, 2004; Xu *et al.*, 2004; Ding *et al.*, 2006; Wu *et al.*, 2009; Nunes and Annunziata, 2017). Thus, multiple downstream effects of proteasome inhibition may contribute to the changes in mRNA levels we observed, with one possible consequence being the impairment of NMD.

Time courses revealed that FVβ-PTC reporter mRNA levels remained relatively constant after 1 h of proteasome inhibition, but started changing as early as after 2 h of treatment (Figure 2B; Supplemental Figure S1D). Importantly, 1 h of proteasome inhibition still increased polyubiquitinated protein levels corresponding to the accumulation of undergraded proteasomal clients (Supplemental Figure S1D). Based on these findings, we investigated the effect of 1 h of proteasome inhibition on FVβ-PTC and FVβ-TC protein levels before changes in mRNA levels could be detected. To accommodate the acute inhibitor treatment and bypass limitations of immunoblotting steady-state protein levels, we used pulse radiolabeling with ³⁵S-labeled methionine coupled with denaturing anti-FLAG immunoprecipitations (IPs) to measure nascent reporter protein levels without and with proteasome inhibition for 1 h. We adjusted for the difference in FVβ-TC and FVβ-PTC expression levels by diluting the input lysates of FVβ-TC reporter cells fourfold for IP. While the level of newly synthesized FVβ-TC protein changed minimally with proteasome inhibition, the level of newly synthesized FVβ-PTC protein increased by ~30% with proteasome inhibition (Figure 2C). These results indicate that a portion of nascent FVβ-PTC protein is selectively targeted for proteasomal degradation compared with the same protein product synthesized from an mRNA that is not targeted for NMD.

Proteins synthesized from NMD-targeted transcripts are specifically destabilized

The selective stabilization of FVβ-PTC compared with FVβ-TC by proteasome inhibition was specific and reproducible (Figure 2C). However, the relatively small effect size compared with the experimental variability introduced with additional manipulations hampered meaningful mechanistic dissections using solely this biochemical assay. We therefore sought to establish an independent system to validate our findings and facilitate cellular investigations of prematurely terminated polypeptide fates. To do this, we designed dual fluorescent protein reporters (referred to as dFP-TC or dFP-PTC) that replaced the open reading frame of our previously introduced FVβ-TC and FVβ-PTC reporters with mCherry, followed by a P2A sequence to induce ribosome skipping (Kim *et al.*, 2011),

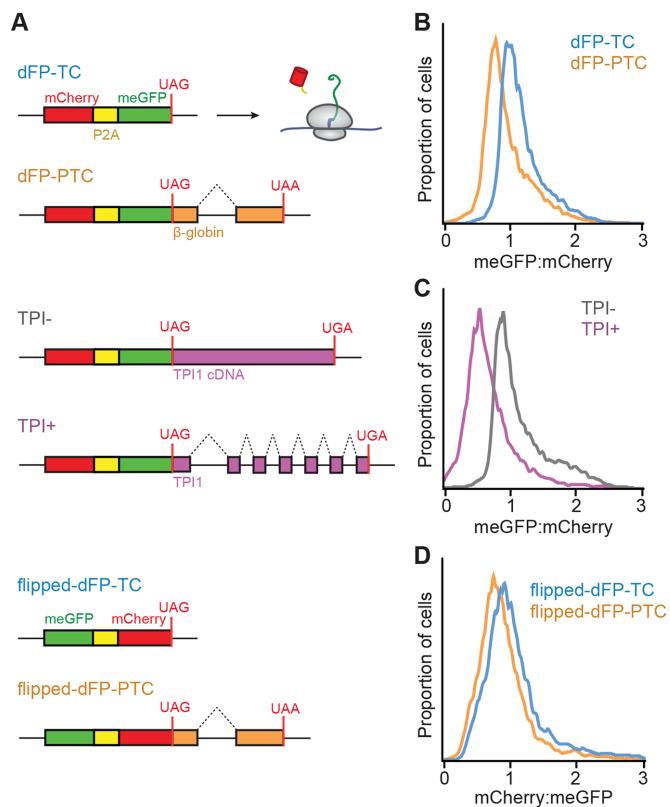


FIGURE 3: Selective destabilization of proteins synthesized from NMD-targeted transcripts. (A) dFP reporter design scheme. Identical protein sequences comprising mCherry, a P2A ribosome skipping sequence, and meGFP are placed before the termination codon of the TC and PTC reporters described in Figure 1A. Translation produces an mCherry molecule that is separated from meGFP before translation termination (right diagram). Dashed lines, constitutive splice sites. The TPI⁻ and TPI⁺ reporters contain the cDNA or genomic sequence of the TPI1 gene without or with six introns downstream of the stop codon, respectively. The flipped-dFP reporters have the opposite order of fluorescent proteins such that an meGFP molecule is synthesized and separated from mCherry before translation termination. (B) Stable expression of the dFP-TC and dFP-PTC reporters as in A was induced in Flp-In T-REx HEK293 cells with 10 ng/ml doxycycline for 4 h before the cells were harvested and analyzed by fluorescence flow cytometry. Shown are the meGFP:mCherry ratios for each population. (C) As in B but for the TPI⁻ and TPI⁺ reporters. (D) As in B, except the mCherry:meGFP ratios are shown for the flipped-dFP reporters.

and monomeric eGFP (meGFP) (Kitajima *et al.*, 2018) (Figure 3A). Translation of either dFP reporter mRNA would produce an mCherry molecule that is released from the ribosome before the ribosome completes synthesis of meGFP. Because ribosomes would arrive at the stop codon bearing only the meGFP nascent chain, any translation termination-associated process would specifically affect meGFP levels, while mCherry levels would serve to normalize for total reporter translation events (Figure 3A).

Using fluorescence flow cytometry to measure meGFP and mCherry levels in cells stably expressing dFP-TC or dFP-PTC, we observed lower meGFP:mCherry ratios in dFP-PTC reporter cells than in dFP-TC reporter cells (Figure 3B). Consistent with ongoing NMD, meGFP and mCherry levels were approximately an order of magnitude lower in dFP-PTC reporter cells than in dFP-TC reporter cells (Supplemental Figure S2A). We observed the same effects with an independent set of dFP reporters in which NMD was elicited by

inserting the triosephosphate isomerase (TPI) gene containing six introns (Boehm *et al.*, 2014; Hoek *et al.*, 2019) after the mCherry-P2A-meGFP sequence (referred to as TPI⁺) compared with a matched control in which the TPI cDNA sequence without any introns was inserted (referred to as TPI⁻) (Figure 3, A and C; Supplemental Figure S2B). TPI⁻ and TPI⁺ not only have identical reading frames but also generate identical mature mRNA sequences. Thus, the only expected difference between these reporters is the deposition of EJC downstream of the termination codon by the splicing of TPI⁺ reporter transcripts that would not be present on TPI⁻ transcripts. These results suggest that proteins synthesized from diverse NMD target transcripts are selectively destabilized.

Effects of expression levels and protein maturation on quantitative fluorescence measurements

The flow cytometry assay provides quantitative single cell measurements instead of population averages, specifically monitors post-translational protein destabilization via the ratio of fluorescent protein levels, and involves fewer experimental manipulations than most biochemical assays. We also excluded reasons that may confound the readouts of this assay, specifically the large difference in the expression levels of the TC and PTC reporters, or potential differences in fluorescent protein maturation and turnover rates. Several observations suggest that these factors do not artifactually bias the central interpretation that premature termination is sufficient to destabilize polypeptides.

We performed the same analysis using cells expressing a TC or PTC reporter in which the order of the fluorescent proteins were switched (i.e., meGFP-P2A-mCherry; referred to as flipped-dFP-TC or flipped-dFP-PTC) and found that the flipped-dFP-PTC reporter cells also showed a lower terminating protein:normalizing protein (in this case, mCherry:meGFP) ratio than flipped-dFP-TC cells (Figure 3D; Supplemental Figure S2C). The difference between the flipped-dFP-TC and flipped-dFP-PTC reporters was slightly smaller, which we reasoned may be due partially to the slower maturation rate of mCherry compared with meGFP (Balleza *et al.*, 2018). Indeed, treating cells with puromycin to inhibit further translation and provide time for the folding of already synthesized proteins increased mCherry fluorescence while meGFP fluorescence was mostly unchanged (Figure 4A; Supplemental Figure S3). These results suggest that on average, more mCherry molecules matured than were turned over during the 1 h incubation with puromycin.

We observed the same trends in mCherry and meGFP levels with puromycin treatment in both PTC and TC reporter cells regardless of the order of the fluorescent proteins in the reporter sequence (Figure 4A; Supplemental Figure S3). Importantly, the PTC reporters had lower ratios of terminating protein to normalizing protein levels compared with the matched TC reporters in all conditions (Figure 4B; Supplemental Figure S3). Thus, while fluorescent protein maturation and turnover rates may affect the magnitude of effects obtained using this assay, controlling for these considerations continues to support a model in which proteins synthesized from NMD targets are selectively destabilized during or after translation.

Finally, to directly test how transcript levels affect the ratiometric readouts, we generated two characterized deletions in the CMV promoter of the dFP-TC reporter, referred to as CMVd1-TC and CMVd3-TC, that reduce expression levels (Figure 4C) (Slater *et al.*, 2008). As expected, TC reporter expression levels decreased progressively with CMV deletions of increasing severity (Figure 4D, left panel). Notably, although CMVd3-TC expression levels were comparable to the matched PTC reporter as judged by RT-qPCR and mCherry levels, the meGFP:mCherry ratios of CMVd1-TC and

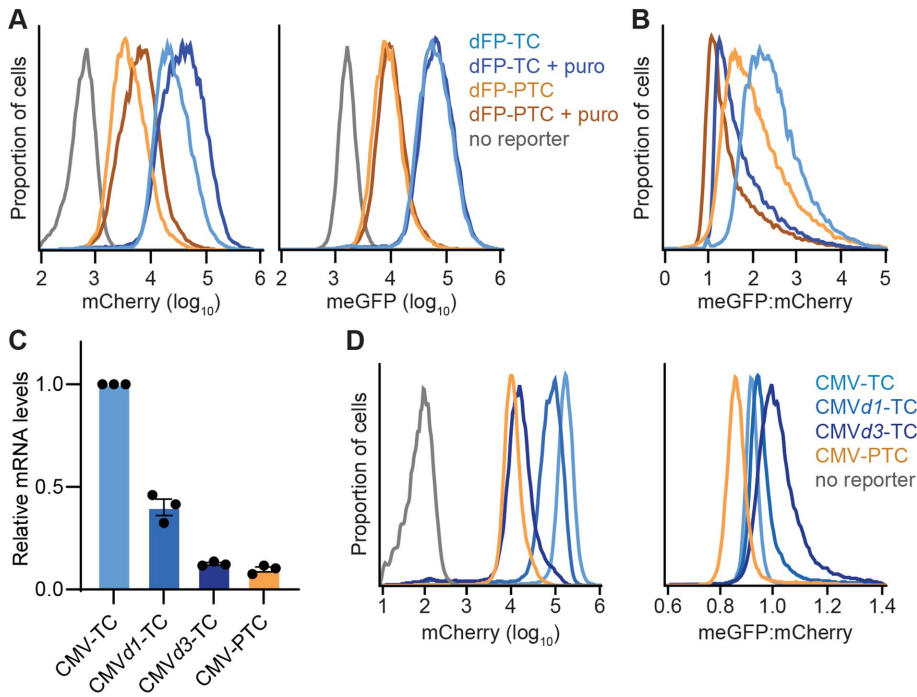


FIGURE 4: Effects of maturation rates and expression level on fluorescence measurements. (A) dFP-TC and dFP-PTC reporter cells were induced with 10 ng/ml doxycycline for 4 h and then treated with 50 μ g/ml puromycin for 1 h after the induction period. Cells were analyzed by fluorescence flow cytometry either before or after the puromycin treatment. mCherry levels (left) and meGFP levels (right) are shown. Cells that do not express a fluorescent reporter are indicated by a gray trace. (B) meGFP:mCherry ratios of puromycin-treated dFP reporter cells as in A. (C) The indicated Flp-In T-REx HEK293 dFP-TC reporter cell lines were generated without or with the indicated deletions (*d1* or *d3*) within the CMV promoter. Reporter expression was induced with 10 ng/ml doxycycline for 24 h, and dFP reporter mRNA levels were analyzed by RT-qPCR and plotted normalized to CMV-TC values. Shown are mean \pm SEM for three replicates. (D) dFP reporter cells as in C were harvested and analyzed by fluorescence flow cytometry. Shown are the mCherry levels (left) and meGFP:mCherry ratio (right) for the indicated populations.

CMVd3-TC were even higher than the unmodified TC reporter (Figure 4D, right panel). Thus, lower expression levels do not account for the decreased fluorescent protein ratios seen with the PTC reporters. Altogether, these experiments present multiple lines of evidence indicating that proteins terminating at PTCs are specifically destabilized.

Depleting NMD factors partially rescues the stability of prematurely terminated polypeptides

Next, we tested how perturbations to the NMD pathway that would increase expression of the PTC reporter affect protein stability. To do this, we first knocked down UPF1 and SMG1. As expected, these knockdowns selectively stabilized dFP-PTC reporter mRNA and protein levels (Figure 5, A and B). Depleting UPF1 or SMG1 also selectively increased the meGFP:mCherry ratios of the dFP-PTC reporter but not of the dFP-TC reporter (Figure 5B; Supplemental Figure S4A). We observed similar increases in the terminating:normalizing protein ratio of the flipped-dFP-PTC reporter up on UPF1 or SMG1 knockdown (Supplemental Figure S4B). In both cases, depleting SMG1 resulted in a stronger rescue of PTC reporter stability than depleting UPF1, even though cellular UPF1 levels were higher in SMG1 knockdown cells than in wild-type cells (Figure 5C). While these differences may be influenced by varying knockdown efficiencies, this observation suggests that UPF1 is involved in, but is not

sufficient to mediate, the degradation of proteins that terminate at a PTC. In contrast, we did not observe any changes in reporter protein stability when we knocked down the E3 ligase Listerin or NEMF, factors in the ribosome-associated quality control (RQC) pathway responsible for degrading nascent proteins on ribosomes that stall during translation elongation (Supplemental Figure S4C). Thus, depleting factors that activate NMD specifically impair the selective destabilization of polypeptides synthesized from PTC-containing transcripts.

Because we observed increased PTC reporter stability by knocking down SMG1, we next examined the effect of SMG1i (Figure 5D), a small molecule inhibitor of SMG1 kinase activity that has previously been shown to inhibit UPF1 phosphorylation (Gopalsamy *et al.*, 2012; Mino *et al.*, 2019; Langer *et al.*, 2021). Consistent with NMD inhibition, treatment with SMG1i specifically increased dFP-PTC reporter levels (Figure 5, E and F). Direct treatment with SMG1i also appeared to increase the meGFP:mCherry ratio of the dFP-PTC reporter (Supplemental Figure S4D). However, unlike the results obtained with knocking down SMG1 and UPF1, the analogous effect was not observed with the flipped-dFP-PTC reporter (Supplemental Figure S4D). We reasoned that this discrepancy may be at least partially due to a stronger influence of fluorescent protein maturation rates during the short 4 h treatment with SMG1i compared with the 72 h time period of siRNA-mediated knockdowns. Indeed, adding a 1 h puromycin treatment revealed that SMG1i had a minimal effect on the terminating:normalizing protein ratios of both dFP-PTC and flipped-dFP-PTC reporters despite increased expression (Figure 5F; Supplemental Figure S4E). In comparison, puromycin treatment did not affect the result of knocking down UPF1 or SMG1 on the terminating:normalizing protein ratio of both the dFP-PTC and the flipped-dFP-PTC reporter cells (Supplemental Figure S4F). Considered together, these results suggest that SMG1 plays a role in destabilizing prematurely terminated polypeptides, but not necessarily through its activity of phosphorylating UPF1 (Figure 5G).

DISCUSSION

Our results indicate that PTC recognition is sufficient to destabilize nascent polypeptides in mammalian cells, adding to a growing collection of evidence suggesting that NMD and protein degradation are linked (Kuroha *et al.*, 2009, 2013; Pradhan *et al.*, 2021; Udy and Bradley, 2021). Identifying the mechanisms that target proteins synthesized from PTC-containing transcripts for proteasomal degradation is an important goal for future studies. These mechanisms may directly involve NMD factors. UPF1 has a RING-like domain that may act as an E3 ubiquitin ligase to mediate protein ubiquitination, the most common signal for proteasomal targeting (Kadlec *et al.*, 2006; Takahashi *et al.*, 2008). UPF1 also has been linked to the destabilization of prematurely terminated nascent proteins in yeast (Kuroha *et al.*, 2009, 2013) and to some proteins in mammalian cells

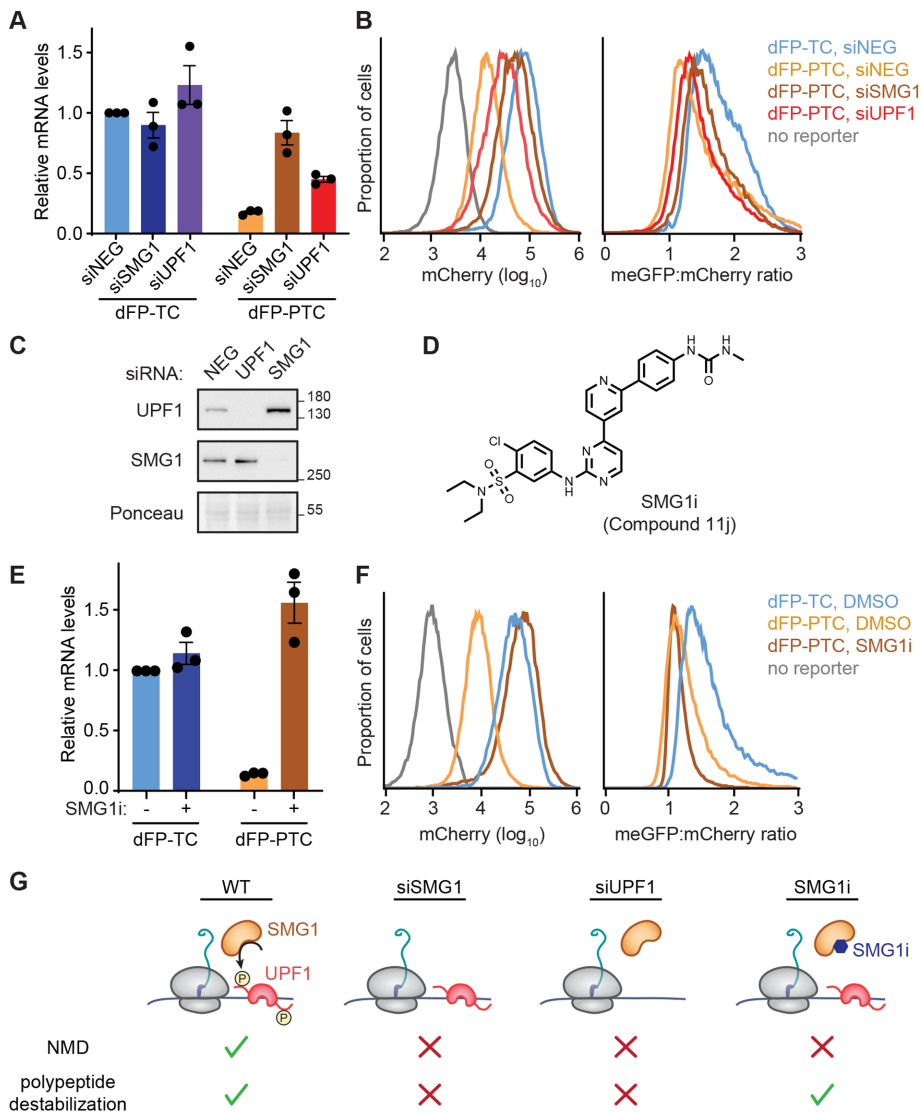


FIGURE 5: Depleting NMD factors impairs selective protein destabilization. (A) dFP reporter mRNA levels measured by RT-qPCR after 72 h of treatment with negative control siRNA (siNEG) or siRNAs to knock down SMG1 (siSMG1) or UPF1 (siUPF1). Shown are mean \pm SEM for three replicates normalized to the dFP-TC siNEG sample. (B) mCherry levels (left) and meGFP:mCherry ratios (right) for the dFP reporter cells as in A. (C) Representative immunoblots of cells treated with control siRNAs (siNEG) or with siRNAs to knock down UPF1 (siUPF1) or SMG1 (siSMG1). (D) Chemical structure of SMG1i. (E) dFP reporter mRNA levels of dFP-TC and dFP-PTC cells induced with 10 ng/ml doxycycline and treated without and with 1 μ M SMG1i for 4 h. Shown are mean \pm SEM for three replicates normalized to the untreated TC sample. (F) mCherry levels (left) and meGFP:mCherry ratios (right) for dFP reporter cells induced with 10 ng/ml doxycycline and treated without or with 1 μ M SMG1i for 4 h, and treated with 50 μ g/ml puromycin for 1 h after the induction period. (G) Summary of NMD, PTC-activated protein degradation and the expected presence of SMG1, UPF1, and/or UPF1 phosphorylation (P) near ribosomes terminating at a PTC in wild-type (WT) cells or cells treated with siSMG1, siUPF1, or SMG1i. Other components involved in PTC recognition, such as translation termination factors and EJC components, are not shown for simplicity.

(Feng *et al.*, 2017; Park *et al.*, 2020). Our results support a role for UPF1 in mediating the destabilization of proteins synthesized from PTC-containing mRNAs. We also observe that SMG1 depletion appears to stabilize proteins synthesized from PTC-containing mRNAs despite increasing UPF1 levels. Because a similar rescue of PTC reporter stability was not seen by inhibiting SMG1 catalytic activity, it is possible that the specific and reciprocal recruitment of SMG1 and

UPF1 to ribosomes terminating at PTCs may play a structural role in the mechanisms that lead to nascent protein destabilization.

Multiple mechanisms also may cooperate to degrade proteins synthesized from NMD-targeted transcripts. For example, although we did not observe a contribution from RQC factors on PTC reporter stability in our study, RQC appears to play a role in degrading at least one prematurely terminated protein in yeast (Pradhan *et al.*, 2021). The involvement of RQC may be consistent with observations suggesting that NMD cooperates with mRNA surveillance mechanisms linked to ribosome stalling (Arribere and Fire, 2018), which may result from slower translation termination at PTCs (Amrani *et al.*, 2004; Peixeiro *et al.*, 2012; Neuyilik *et al.*, 2017) or from translation of mRNAs truncated by SMG6 cleavage (Hoek *et al.*, 2019). Specific substrate features likely influence the involvement of different mechanisms. For example, the location of a PTC determines if a polypeptide is exposed for modification outside of the ribosomal exit tunnel at the point of translation termination and also influences the number and speed of translating ribosomes on the transcript that establish the likelihood of ribosome collisions linked to RQC activation.

Our study also refines the framework for studying the mechanisms that degrade prematurely terminated polypeptides. Numerous challenges currently limit the precision with which this question can be investigated. Low levels of NMD-targeted transcripts hinder biochemical analyses of the resulting polypeptides, and the orders of magnitude differences between the expression levels of NMD-targeted and control transcripts complicate quantitative comparisons. The essentiality of core NMD components and the role that NMD plays in suppressing gene expression also hampers the production of certain knock-out systems (Gurumayum *et al.*, 2021), and prolonged depletion of NMD components may introduce unpredictable off-target effects. Thus, the cellular manipulations and experimental readouts available to study these processes remain relatively indirect. Our observations additionally identify possible confounding effects of proteasome inhibition on NMD in mammalian cells that may add caution to interpretations related to protein degradation and inform the design of future studies.

In comparison, proteasome inhibitors appear to have minimal effects on NMD-targeted mRNA levels in prior studies in yeast (Kuroha *et al.*, 2009). Thus, the generality and potential mechanisms that lead to changes in PTC-containing transcript levels on proteasome inhibition remain to be fully determined.

Moreover, our cellular reporters enable further investigations into the selective degradation of proteins that terminate at a PTC in mammalian cells. Reporters optimized for biochemical or cellular assays allowed us to leverage multiple readouts to control for limitations of individual systems while probing a low-abundance cellular process. Other quantitative NMD reporters recently established in mammalian cells assay protein levels by measuring distinct enzymatic activities appended to different protein sequences (Udy and Bradley, 2021). While these reporters may be influenced by different intrinsic stabilities, enzyme maturation rates, and/or catalytic activity, they reassuringly also support a model in which multiple mechanisms act to limit the accumulation of prematurely terminated proteins. In our study, the matched reporter sequences control for possible contributions of uncharacterized properties of different protein sequences to the stability of prematurely terminated polypeptides. In addition, biochemical measurements of nascent protein levels with proteasome inhibitors and the analysis of dFP reporters designed to uncouple effects of protein synthesis and degradation specifically implicate a role for protein degradation in preventing prematurely terminated protein accumulation. These findings push forward the development of more precise experimental strategies, such as identifying tractable substrates for cell-free reconstitutions, to dissect the cross-talk between these mRNA and protein quality control mechanisms.

MATERIALS AND METHODS

[Request a protocol](#) through *Bio-protocol*.

Plasmids and antibodies

A pcDNA5/FRT/TO-based plasmid containing the β -globin gene (pcDNA5/FRT/TO-globin_del5UTR_PTC39-xrRNA-4H) was a gift from Niels Gehring (Boehm *et al.*, 2016). The FV β sequence (Shao *et al.*, 2013, 2015, 2016) was amplified by PCR and inserted into PCR-linearized pcDNA5- β -globin to replace either the entire β -globin sequence or the coding region for the first 39 amino acids using Gibson assembly (New England Biolabs) to generate the FV β -TC and FV β -PTC constructs, respectively.

For fluorescent protein reporter constructs (dFP and flipped-dFP), mCherry and meGFP sequences were amplified by PCR (Juzskiewicz and Hegde, 2017), and the sequence of the first fluorescent protein was inserted into PCR-linearized TC and PTC constructs using Gibson assembly. The P2A sequence was added by Phusion mutagenesis, and then the insert encoding the second fluorescent protein was added after the P2A sequence using Gibson assembly.

For TPI $^-$ and TPI $^+$ reporters, the respective inserts were amplified by PCR from a gBlock (Integrated DNA Technologies) encoding the human TPI1 gene without introns or from a plasmid encoding the human TPI1 gene with introns (pCI-TPI-WT-4H), kindly provided by Niels Gehring. The inserts were added into the PCR-linearized dFP-TC construct after the stop codon using Gibson assembly.

Primary antibodies and dilutions used for immunoblotting were as follows: anti-FLAG M2 mouse antibody (Sigma-Aldrich, F1804) at 1:5000, anti-UPF1 rabbit antibody (Abcam, ab86057) at 1:10,000, anti-ubiquitin (P4D1) rabbit antibody (Santa Cruz, sc-8017) at 1:200, anti-SMG1 rabbit antibody (Abcam, ab151730) at 1:1000, anti-NEMF rabbit antibody as previously described (Shao *et al.*, 2015) at 1:500, and anti-Ltn1 rabbit antibody (Abcam, ab104375) at 1:500. Horseradish peroxidase (HRP)-conjugated anti-mouse (Jackson ImmunoResearch Laboratories, 115-035-003) and anti-rabbit (Jackson ImmunoResearch Laboratories, 111-035-003) secondary antibodies were used at 1:5000.

Cell culture, transient transfections, and cell line generation

All cells were cultured at 37°C and 5% CO₂ in DMEM with high glucose (4.5 g/l), GlutaMAX, and pyruvate (110 mg/l) (Life Technologies 10569044) supplemented with 10% fetal bovine serum (FBS). Transient transfections of HEK293 cells were performed using *TransIT-293* (Mirus) according to the manufacturer's instructions. To generate stable cell lines, Flp-In T-REx 293 cells were cotransfected with the pcDNA5/FRT/TO plasmid containing the reporter gene and pOG44 encoding for the Flp recombinase in a 1:1 ratio using *TransIT-293* (Mirus) following the manufacturer's instructions. Two days after transfection, cells were placed under selection and maintained with 10 μ g/ml blasticidin S HCl (Life Technologies) and 100 μ g/ml hygromycin B (Life Technologies). Reporter expression was induced with 10 ng/ml doxycycline hyclate (Sigma-Aldrich) for 4 h for fluorescent reporters or 24 h for FV β reporters prior to analysis, unless otherwise indicated.

siRNA-mediated knockdowns and small molecule treatments

All knockdowns and small molecule treatments were performed on cells seeded in the absence of antibiotics. siRNA-mediated knockdowns were performed by reverse transfection in 6-well plates with 25 pmol siRNA using Lipofectamine RNAiMAX (Invitrogen) following the manufacturer's instructions. For each treatment condition, 5 \times 10⁵ cells were seeded in 6-well plates and incubated for 72 h after transfection. The following siRNA sense sequences were used: siNEG (SN-1003, Bioneer); siUPF1 (Bioneer), 5'-GAUGCAGUCCG CUCCAUU(dTdT)-3' (Mendell *et al.*, 2002); siSMG1 (Bioneer), 5'-GUGUAUGUGCGCCAAAGUA(dTdT)-3' (Usuki *et al.*, 2006); siNEMF SmartPool (Dharmacon), 5'-CGUUAGAGGGAAAGGAUAA (UU)-3', 5'-AAUUAUAGGUGGACGAGAU(UU)-3', 5'-CCUACAAA-UAGUUGACAGA(UU)-3', 5'-GAAAAUGGAUUCUCGGGUA(UU)-3'; siLtn1 (Dharmacon), 5'-GCGAAAGGAUGCUUGC UAA(UU)-3'. Due to increased toxicity observed with siUPF1, the number of cells used for siUPF1 was 1.5 \times the amount used for the other siRNAs.

Proteasome inhibition was with 0.5 μ M bortezomib (LC Laboratories) and 0.5 μ M epoxomicin (ApexBio), unless otherwise indicated. SMG1i treatments were for 4 h with 1 μ M SMG1i. Puromycin treatments were for 1 h with 50 μ g/ml puromycin (Life Technologies).

Immunoblotting and radiolabeling pulse assays

For immunoblotting, cells were harvested in cold phosphate-buffered saline (PBS) and pelleted by centrifugation at 1000 \times g for 5 min at 4°C. The pellet was resuspended in lysis buffer [50 mM HEPES, pH 7.5, 100 mM KOAc, 5 mM Mg(OAc)₂, 0.025% digitonin, 1 \times cOmplete protease inhibitor cocktail (Roche), 1 mM dithiothreitol (DTT)] and left on ice for 10 min. The lysate was clarified by centrifugation at 21,130 \times g for 10 min at 4°C. Protein concentrations were normalized according to absorbance at 280 nm, and normalized lysates were denatured by boiling for 5 min in protein sample buffer before SDS-PAGE and wet-transferred to 0.2- μ m nitrocellulose membranes. Blots were incubated with primary antibodies in 5% milk overnight at 4°C and with HRP-conjugated secondary antibodies for 1 h at room temperature. Densitometry was performed using ImageJ.

For radiolabeling pulse assays, cells were detached using 0.25% trypsin-EDTA, resuspended in complete growth medium, and pelleted by centrifugation at 500 \times g for 3 min. The cells were washed in PBS and resuspended in complete growth medium containing dialyzed FBS. For each treatment condition, 1 \times 10⁶ cells were dispensed into a 1.5-ml tube, pelleted at 500 \times g for 30 s, and resuspended in 18 μ l of complete growth medium containing

dialyzed FBS and either DMSO or 0.5 μM bortezomib and 0.5 μM epoxomicin. The tubes were placed in a 37°C water bath for 10 min before the addition of 2 μl of EasyTag L-[³⁵S]-methionine (PerkinElmer) and an additional 1 h incubation at 37°C. Radiolabeling reactions were stopped by placing the tubes on ice and adding 500 μl cold PBS. The cells were pelleted by centrifugation at 500 \times g for 30 s at 4°C, lysed in 25 μl lysis buffer, and clarified by centrifugation at 21,130 \times g for 10 min at 4°C. For denaturing IPs, 21 μl of clarified lysate was mixed with an equal volume of 2% SDS in 0.1 M Tris, pH 8.5, and boiled for 5 min; 2 μl was taken for input samples. Ten microliters (for FV β -TC) or 40 μl (for FV β -PTC) of denatured lysate were incubated with 1 ml IP buffer [50 mM HEPES, pH 7.5, 100 mM KOAc, 5 mM Mg(OAc)₂, 1% Triton X-100, 1 mM DTT] and 10 μl packed volume of equilibrated anti-FLAG M2 agarose resin (Sigma-Aldrich) for 1 h at 4°C. The beads were washed 3 \times with IP buffer, eluted with 20 μl 2 \times protein sample buffer, and boiled for 5 min before SDS-PAGE, Coomassie staining with ethanol fixation, and drying on filter paper. Autoradiography was performed using a phosphor screen (Fujifilm) on an Amersham Typhoon imager. Densitometry was performed using ImageQuant TL software.

RT-qPCR

Cells were collected in cold PBS, pelleted by centrifugation at 1000 \times g for 5 min at 4°C, and resuspended in Buffer RLT (QIAGEN) with 1% β -mercaptoethanol added. Cells were lysed by shaking in a thermomixer at 1400 rpm for 15 min, and the lysates were frozen at -80°C until RNA extraction. RNA extraction was performed using the RNeasy Mini kit (QIAGEN). The eluted RNA was treated with RNase-free DNase (QIAGEN) and reisolated using the RNeasy Mini Kit. Reverse transcription of 0.5 μg RNA was performed using oligo(dT)₂₀ primers and the SuperScript III First-Strand Synthesis System (Invitrogen) according to the manufacturer's instructions, except that DTT was omitted from the reactions. The resulting cDNA was diluted 1:200 and mixed with SYBR Green Master Mix (Applied Biosystems) and 300 nM each of forward and reverse primers. The following primers were used: SRP14-forward 5'-GAGAGCG-AGCAGTTCCTGAC-3'; SRP14-reverse 5'-GTTTGGTTTCGAC-GTCATACT-3'; FV β -forward 5'-CAAGGATGACGATGACAAGG-3'; FV β -reverse 5'-CTGTTTCCACAAGGGCAAGT-3'; GFP-forward 5'-CGACCACTACCAGCAGAACA-3'; GFP-reverse 5'-GTGATCGC-GCTTCTCGTT-3'. RT-qPCR was performed using the QuantStudio 7 Pro real-time PCR system. Amplification efficiencies for each primer set were assessed using a fourfold dilution series. For each biological replicate, the average C_T (threshold cycle) was calculated from three technical replicates. Fold changes were calculated using the $\Delta\Delta\text{C}_T$ method, correcting for amplification efficiency (Livak and Schmittgen, 2001; Pfaffl, 2001). SRP14 was used as the reference gene. Data from three biological replicates were analyzed using GraphPad Prism 9.

Fluorescence flow cytometry

Cells were detached using 0.25% trypsin-EDTA, resuspended in complete growth medium, and pelleted by centrifugation at 500 \times g for 3 min. The cells were then washed in PBS and resuspended in 1% FBS in PBS. Cells were filtered through a 35- μm mesh strainer and kept on ice. Data were collected on 30,000 cells per sample on an Attune NxT flow cytometer. Data analysis was performed in FlowJo. Background cellular fluorescence was defined as the median fluorescence values of Flp-In T-REx 293 cells expressing no reporter. The meGFP:mCherry ratio for each cell was calculated by dividing the background-subtracted meGFP fluorescence value by the background-subtracted mCherry fluorescence value.

ACKNOWLEDGMENTS

We thank Niels Gehring for plasmids encoding β -globin and TPI1; Robert Bridges, Rosalind Franklin University of Medicine and Science, and the Cystic Fibrosis Foundation for SMG1i; Kenneth Gray and Sookhee Park for help and training with flow cytometry; Tom Rapoport for critical reading; and Dan Finley, Brian Liao, Wade Harper, Yan Cheng, and Shao lab members for helpful discussions. RT-qPCR was performed at the HMS ICCB-Longwood Screening Facility. V.C. was supported in part by an NDSEG fellowship; Q.F. was supported in part by a Jane Coffin Childs Fellowship. This work was supported by the Cystic Fibrosis Foundation, the Vallee Foundation, a Packard Fellowship, and National Institutes of Health DP2GM137415.

REFERENCES

- Amrani N, Ganesan R, Kervestin S, Mangus DA, Ghosh S, Jacobson A (2004). A faux 3'-UTR promotes aberrant termination and triggers nonsense-mediated mRNA decay. *Nature* 432, 112–118.
- Arribere JA, Fire AZ (2018). Nonsense mRNA suppression via nonstop decay. *Elife* 7, e33292.
- Balleza E, Kim JM, Cluzel P (2018). Systematic characterization of maturation time of fluorescent proteins in living cells. *Nat Methods* 15, 47–51.
- Belgrader P, Cheng J, Maquat LE (1993). Evidence to implicate translation by ribosomes in the mechanism by which nonsense codons reduce the nuclear level of human triosephosphate isomerase mRNA. *Proc Natl Acad Sci USA* 90, 482–486.
- Boehm V, Gerbracht JV, Marx M-C, Gehring NH (2016). Interrogating the degradation pathways of unstable mRNAs with XRN1-resistant sequences. *Nat Commun* 7, 13691.
- Boehm V, Haberman N, Ottens F, Ule J, Gehring NH (2014). 3' UTR length and messenger ribonucleoprotein composition determine endocleavage efficiencies at termination codons. *Cell Rep* 9, 555–568.
- Bühler M, Steiner S, Mohn F, Paillusson A, Mühlemann O (2006). EJC-independent degradation of nonsense immunoglobulin- μ mRNA depends on 3' UTR length. *Nat Struct Mol Biol* 13, 462–464.
- Carter MS, Doskow J, Morris P, Li S, Nhim RP, Sandstedt S, Wilkinson MF (1995). A regulatory mechanism that detects premature nonsense codons in T-cell receptor transcripts in vivo is reversed by protein synthesis inhibitors in vitro. *J Biol Chem* 270, 28995–29003.
- Chakrabarti S, Bonneau F, Schuessler S, Eppinger E, Conti E (2014). Phospho-dependent and phospho-independent interactions of the helicase UPF1 with the NMD factors SMG5-SMG7 and SMG6. *Nucleic Acids Res* 42, 9447–9460.
- Chang JC, Kan YW (1979). beta 0 thalassemia, a nonsense mutation in man. *Proc Natl Acad Sci USA* 76, 2886–2889.
- Cho H, Han S, Choe J, Park SG, Choi SS, Kim YK (2013). SMG5-PNRC2 is functionally dominant compared with SMG5-SMG7 in mammalian nonsense-mediated mRNA decay. *Nucleic Acids Res* 41, 1319–1328.
- Cowan JL, Morley SJ (2004). The proteasome inhibitor, MG132, promotes the reprogramming of translation in C2C12 myoblasts and facilitates the association of hsp25 with the eIF4F complex. *Eur J Biochem* 271, 3596–3611.
- Ding Q, Dimayuga E, Markesbery WR, Keller JN (2006). Proteasome inhibition induces reversible impairments in protein synthesis. *FASEB J* 20, 1055–1063.
- Dostie J, Dreyfuss G (2002). Translation Is Required to Remove Y14 from mRNAs in the Cytoplasm. *Curr Biol* 12, 1060–1067.
- Eberle AB, Lykke-Andersen S, Mühlemann O, Jensen TH (2009). SMG6 promotes endonucleolytic cleavage of nonsense mRNA in human cells. *Nat Struct Mol Biol* 16, 49–55.
- Eberle AB, Stalder L, Mathys H, Orozco RZ, Mühlemann O (2008). Posttranscriptional gene regulation by spatial rearrangement of the 3' untranslated region. *PLoS Biol* 6, 849–859.
- Feng Q, Jagannathan S, Bradley RK (2017). The RNA surveillance factor UPF1 represses myogenesis via its E3 ubiquitin ligase activity. *Mol Cell* 67, 239–251.e6.
- García-Moreno JF, Romão L (2020). Perspective in alternative splicing coupled to nonsense-mediated mRNA decay. *Int J Mol Sci* 21, 9424.
- Gehring NH, Lamprinaki S, Kulozik AE, Hentze MW (2009). Disassembly of exon junction complexes by PYM. *Cell* 137, 536–548.
- Gopalsamy A, Bennett EM, Shi M, Zhang W-G, Bard J, Yu K (2012). Identification of pyrimidine derivatives as hSMG-1 inhibitors. *Bioorg Med Chem Lett* 22, 6636–6641.

- Gurumayum S, Jiang P, Hao X, Campos TL, Young ND, Korhonen PK, Gasser RB, Bork P, Zhao X-M, He L, et al. (2021). OGEE v3: Online GEne Essentiality database with increased coverage of organisms and human cell lines. *Nucleic Acids Res* 49, D998–D1003.
- Hauer C, Sieber J, Schwarzl T, Hollerer I, Curk T, Alleaume A-M, Hentze MW, Kulozik AE (2016). Exon junction complexes show a distributional bias toward alternatively spliced mRNAs and against mRNAs coding for ribosomal proteins. *Cell Rep* 16, 1588–1603.
- Hoek TA, Khuperkar D, Lindeboom RGH, Sonneveld S, Verhagen BMP, Boersma S, Vermeulen M, Tanenbaum ME (2019). Single-molecule imaging uncovers rules governing nonsense-mediated mRNA decay. *Mol Cell* 75, 324–339.e11.
- Hogg JR, Goff SP (2010). Upf1 senses 3'UTR length to potentiate mRNA decay. *Cell* 143, 379–389.
- Huntzinger E, Kashima I, Fauser M, Sauliere J, Izaurralde E (2008). SMG6 is the catalytic endonuclease that cleaves mRNAs containing nonsense codons in metazoan. *RNA* 14, 2609–2617.
- Hwang J-W, Sato H, Tang Y-L, Matsuda D, Maquat LE (2010). UPF1 association with the cap-binding protein, CBP80, promotes nonsense-mediated mRNA decay at two distinct steps. *Mol Cell* 39, 396–409.
- Ishigaki Y, Li X, Serin G, Maquat LE (2001). Evidence for a pioneer round of mRNA translation: mRNAs subject to nonsense-mediated decay in mammalian cells are bound by CBP80 and CBP20. *Cell* 106, 607–617.
- Jonas S, Weichenrieder O, Izaurralde E (2013). An unusual arrangement of two 14-3-3-like domains in the SMG5-SMG7 heterodimer is required for efficient nonsense-mediated mRNA decay. *Genes Dev* 27, 211–225.
- Juszkiewicz S, Hegde RS (2017). Initiation of quality control during poly(A) translation requires site-specific ribosome ubiquitination. *Mol Cell* 65, 743–750.e4.
- Kadlec J, Guilligay D, Ravelli RB, Cusack S (2006). Crystal structure of the UPF2-interacting domain of nonsense-mediated mRNA decay factor UPF1. *RNA* 12, 1817–1824.
- Kashima I, Yamashita A, Izumi N, Kataoka N, Morishita R, Hoshino S, Ohno M, Dreyfuss G, Ohno S (2006). Binding of a novel SMG-1-Upf1-eRF1-eRF3 complex (SURF) to the exon junction complex triggers Upf1 phosphorylation and nonsense-mediated mRNA decay. *Genes Dev* 20, 355–367.
- Kim JH, Lee S-R, Li L-H, Park H-J, Park J-H, Lee KY, Kim M-K, Shin BA, Choi S-Y (2011). High cleavage efficiency of a 2A peptide derived from porcine teschovirus-1 in human cell lines, zebrafish and mice. *PLoS One* 6, e18556.
- Kisselev AF, Goldberg AL (2001). Proteasome inhibitors: from research tools to drug candidates. *Chem Biol* 8, 739–758.
- Kitajima T, Xue W, Liu Y-S, Wang C-D, Liu S-S, Fujita M, Gao X-D (2018). Construction of green fluorescence protein mutant to monitor STT3B-dependent N-glycosylation. *FEBS J* 285, 915–928.
- Kuroha K, Ando K, Nakagawa R, Inada T (2013). The Upf factor complex interacts with aberrant products derived from mRNAs containing a premature termination codon and facilitates their proteasomal degradation. *J Biol Chem* 288, 28630–28640.
- Kuroha K, Tatematsu T, Inada T (2009). Upf1 stimulates degradation of the product derived from aberrant messenger RNA containing a specific nonsense mutation by the proteasome. *EMBO Rep* 10, 1265–1271.
- Kurosaki T, Popp MW, Maquat LE (2019). Quality and quantity control of gene expression by nonsense-mediated mRNA decay. *Nat Rev Mol Cell Biol* 20, 406–420.
- Langer LM, Bonneau F, Gat Y, Conti E (2021). Cryo-EM reconstructions of inhibitor-bound SMG1 kinase reveal an autoinhibitory state dependent on SMG8. *BioRxiv*, 2021.07.28.454180.
- Le Hir H, Gatfield D, Izaurralde E, Moore MJ (2001). The exon-exon junction complex provides a binding platform for factors involved in mRNA export and nonsense-mediated mRNA decay. *EMBO J* 20, 4987–4997.
- Lim S, Mullins JJ, Chen CM, Gross KW, Maquat LE (1989). Novel metabolism of several beta zero-thalassaemic beta-globin mRNAs in the erythroid tissues of transgenic mice. *EMBO J* 8, 2613–2619.
- Lindeboom RGH, Vermeulen M, Lehner B, Supek F (2019). The impact of nonsense-mediated mRNA decay on genetic disease, gene editing and cancer immunotherapy. *Nat Genet* 51, 1645–1651.
- Livak KJ, Schmittgen TD (2001). Analysis of relative gene expression data using real-time quantitative PCR and the 2(-Delta Delta C(T)) method. *Methods* 25, 402–408.
- Loh B, Jonas S, Izaurralde E (2013). The SMG5-SMG7 heterodimer directly recruits the CCR4-NOT deadenylase complex to mRNAs containing nonsense codons via interaction with POP2. *Genes Dev* 27, 2125–2138.
- Losson R, Lacroute F (1979). Interference of nonsense mutations with eukaryotic messenger RNA stability. *Proc Natl Acad Sci USA* 76, 5134–5137.
- Lykke-Andersen S, Chen Y, Ardal BR, Lilje B, Waage J, Sandelin A, Jensen TH (2014). Human nonsense-mediated RNA decay initiates widely by endonucleolysis and targets snoRNA host genes. *Genes Dev* 28, 2498–2517.
- Lykke-Andersen J, Shu M-D, Steitz JA (2000). Human Upf proteins target an mRNA for nonsense-mediated decay when bound downstream of a termination codon. *Cell* 103, 1121–1131.
- Maquat LE, Kinniburgh AJ, Rachmilewitz EA, Ross J (1981). Unstable beta-globin mRNA in mRNA-deficient beta0 thalassemia. *Cell* 27, 543–553.
- Mendell JT, ap Rhys CMJ, Dietz HC (2002). Separable roles for rent1/hUpf1 in altered splicing and decay of nonsense transcripts. *Science* 298, 419–422.
- Mendell JT, Sharifi NA, Meyers JL, Martinez-Murillo F, Dietz HC (2004). Nonsense surveillance regulates expression of diverse classes of mammalian transcripts and mutes genomic noise. *Nat Genet* 36, 1073–1078.
- Mimnaugh EG, Chen HY, Davie JR, Celis JE, Neckers L (1997). Rapid deubiquitination of nucleosomal histones in human tumor cells caused by proteasome inhibitors and stress response inducers: effects on replication, transcription, translation, and the cellular stress response. *Biochemistry* 36, 14418–14429.
- Mino T, Iwai N, Endo M, Inoue K, Akaki K, Hia F, Uehata T, Emura T, Hidaka K, Suzuki Y, et al. (2019). Translation-dependent unwinding of stem-loops by UPF1 licenses Regnase-1 to degrade inflammatory mRNAs. *Nucleic Acids Res* 47, 8838–8859.
- Nagy E, Maquat LE (1998). A rule for termination-codon position within intron-containing genes: when nonsense affects RNA abundance. *Trends Biochem Sci* 23, 198–199.
- Nasif S, Contu L, Mühlemann O (2018). Beyond quality control: The role of nonsense-mediated mRNA decay (NMD) in regulating gene expression. *Semin Cell Dev Biol* 75, 78–87.
- Neu-Yilik G, Raimondeau E, Eliseev B, Yeramala L, Amthor B, Deniaud A, Huard K, Kerschgens K, Hentze MW, Schaffitzel C, et al. (2017). Dual function of UPF3B in early and late translation termination. *EMBO J* 36, 2968–2986.
- Nguyen AT, Prado MA, Schmidt PJ, Sendamarai AK, Wilson-Grady JT, Min M, Campagna DR, Tian G, Shi Y, Dederer V, et al. (2017). UBE2O remodels the proteome during terminal erythroid differentiation. *Science* 357, eaan0218.
- Nunes AT, Annunziata CM (2017). Proteasome Inhibitors: Structure and Function. *Semin Oncol* 44, 377–380.
- Ohnishi T, Yamashita A, Kashima I, Schell T, Anders KR, Grimson A, Hachiya T, Hentze MW, Anderson P, Ohno S (2003). Phosphorylation of hUPF1 induces formation of mRNA surveillance complexes containing hSMG-5 and hSMG-7. *Mol Cell* 12, 1187–1200.
- Okada-Katsuhata Y, Yamashita A, Kutsuzawa K, Izumi N, Hirahara F, Ohno S (2012). N- and C-terminal Upf1 phosphorylations create binding platforms for SMG-6 and SMG-5:SMG-7 during NMD. *Nucleic Acids Res* 40, 1251–1266.
- Ottens F, Boehm V, Sibley CR, Ule J, Gehring NH (2017). Transcript-specific characteristics determine the contribution of endo- and exonucleolytic decay pathways during the degradation of nonsense-mediated decay substrates. *RNA* 23, 1224–1236.
- Park Y, Park J, Hwang HJ, Kim B, Jeong K, Chang J, Lee J-B, Kim YK (2020). Nonsense-mediated mRNA decay factor UPF1 promotes aggresome formation. *Nat Commun* 11, 3106.
- Peixeiro I, Inácio Â, Barbosa C, Silva AL, Liebhaber SA, Romão L (2012). Interaction of PABPC1 with the translation initiation complex is critical to the NMD resistance of AUG-proximal nonsense mutations. *Nucleic Acids Res* 40, 1160–1173.
- Pfaffl MW (2001). A new mathematical model for relative quantification in real-time RT-PCR. *Nucleic Acids Res* 29, e45.
- Pradhan AK, Kandasamy G, Chatterjee U, Bharadwaj A, Mathew SJ, Dohmen RJ, Palanimurugan R (2021). Ribosome-associated quality control mediates degradation of the premature translation termination product Orf1p of ODC antizyme mRNA. *FEBS Lett* 595, 2015–2033.
- Saltzman AL, Kim YK, Pan Q, Fagnani MM, Maquat LE, Blencowe BJ (2008). Regulation of multiple core spliceosomal proteins by alternative splicing-coupled nonsense-mediated mRNA decay. *Mol Cell Biol* 28, 4320–4330.
- Saulière J, Murigneux V, Wang Z, Marquet E, Barbosa I, Le Tonquèze O, Audic Y, Paillard L, Crollius HR, Le Hir H (2012). CLIP-seq of eIF4AIII reveals transcriptome-wide mapping of the human exon junction complex. *Nat Struct Mol Biol* 19, 1124–1131.
- Schmidt SA, Foley PL, Jeong D-H, Rymarquis LA, Doyle F, Tenenbaum SA, Belasco JG, Green PJ (2015). Identification of SMG6 cleavage sites and

- a preferred RNA cleavage motif by global analysis of endogenous NMD targets in human cells. *Nucleic Acids Res* 43, 309–323.
- Shao S, Brown A, Santhanam B, Hegde RS (2015). Structure and assembly pathway of the ribosome quality control complex. *Mol Cell* 57, 433–444.
- Shao S, Murray J, Brown A, Taunton J, Ramakrishnan V, Hegde RS (2016). Decoding mammalian ribosome-mRNA states by translational GTPase complexes. *Cell* 167, 1229–1240.e15.
- Shao S, von der Malsburg K, Hegde RS (2013). Listerin-dependent nascent protein ubiquitination relies on ribosome subunit dissociation. *Mol Cell* 50, 637–648.
- Singh G, Rebbapragada I, Lykke-Andersen J (2008). A competition between stimulators and antagonists of Upf complex recruitment governs human nonsense-mediated mRNA decay. *PLoS Biol* 6, 860–871.
- Slater M, Hartzell D, Hartnett J, Wheeler S, Stecha P, Karassina N (2008). Achieve the protein expression level you need with the mammalian HaloTag 7 flexi vectors. *Promega Notes* 100, 16–18.
- Takahashi S, Araki Y, Ohya Y, Sakuno T, Hoshino S-I, Kontani K, Nishina H, Katada T (2008). Upf1 potentially serves as a RING-related E3 ubiquitin ligase via its association with Upf3 in yeast. *RNA* 14, 1950–1958.
- Toma KG, Rebbapragada I, Durand S, Lykke-Andersen J (2015). Identification of elements in human long 3' UTRs that inhibit nonsense-mediated decay. *RNA* 21, 887–897.
- Trcek T, Sato H, Singer RH, Maquat LE (2013). Temporal and spatial characterization of nonsense-mediated mRNA decay. *Genes Dev* 27, 541–551.
- Udy DB, Bradley RK (2021). Nonsense-mediated mRNA decay utilizes complementary mechanisms to suppress mRNA and protein accumulation. *BioRxiv*, [https://doi:10.1101/2021.05.24.445486v1](https://doi.org/10.1101/2021.05.24.445486v1).
- Usuki F, Yamashita A, Kashima I, Higuchi I, Osame M, Ohno S (2006). Specific inhibition of nonsense-mediated mRNA decay components, SMG-1 or Upf1, rescues the phenotype of Ullrich disease fibroblasts. *Mol Ther* 14, 351–360.
- Weischenfeldt J, Waage J, Tian G, Zhao J, Damgaard I, Jakobsen JS, Kristiansen K, Krogh A, Wang J, Porse BT (2012). Mammalian tissues defective in nonsense-mediated mRNA decay display highly aberrant splicing patterns. *Genome Biol* 13, R35.
- Wu WKK, Volta V, Cho CH, Wu YC, Li HT, Yu L, Li ZJ, Sung JY (2009). Repression of protein translation and mTOR signaling by proteasome inhibitor in colon cancer cells. *Biochem Biophys Res Commun* 386, 598–601.
- Xu Q, Farah M, Webster JM, Wojcikiewicz RJH (2004). Bortezomib rapidly suppresses ubiquitin thiolesterification to ubiquitin-conjugating enzymes and inhibits ubiquitination of histones and type I inositol 1,4,5-trisphosphate receptor. *Mol Cancer Ther* 3, 1263–1269.
- Yi Z, Sanjeev M, Singh G (2021). The branched nature of the nonsense-mediated mRNA decay pathway. *Trends Genet* 37, 143–159.